Variability trend in the scale-free fluctuation of economic and market data

D. C. Lin
Department of Mechanical and Industrial Engineering, Ryerson University, Toronto, Ontario, Canada M5B 2K3

(Received 19 November 2008; revised manuscript received 20 February 2009; published 9 June 2009)

Recurring trending feature of a particular duration or size can normally be observed in the scale-free fluctuation of economic and market data. While it contradicts the notion of being scale free, trends are generally believed to exist. From the explicit result of multiplicative cascade and empirical evidence, we show the presence of local cascades underlying the recurring trend and such characteristic is in fact an integral part rather than an aberration of the scale-free fluctuation.

DOI: 10.1103/PhysRevE.79.066104 PACS number(s): 89.65.Gh, 05.45.Tp, 89.75.Da, 05.45.Df

I. INTRODUCTION

Complex dynamics in biological [1] and financial systems [2–10] are commonly found to exhibit scale-free or fractal fluctuation that possesses no reference scale for characterization. However, it is not uncommon to observe in such fluctuations recurring trends of particular duration and size, suggesting the contrary of the scale-free notion. These seemingly conflicting views have led to the precarious nature of trend. Adding to the perception is also the intermittent character of the trend that does not register specific Fourier mode(s). For example, consider the monthly U.S. unemployment rate (UR) in Fig. 1(a). Although the economic downturn is seen to recur with a particular temporal pattern, UR is described by a $1/f$-like power-law spectrum. Indeed, the fluctuation of economic and market data provides the prime example of the sort, from the well-studied leverage effect [11,12] to the less understood "end-of-month-return" (EOMR) phenomenon [13,14] [Fig. 1(b)], where recurring trends and scale-free characteristics are both believed to exist.

In this work, we attempt to define and analyze potential trending feature in the scale-free fluctuation of economic and market data. By systematically comparing past and future fluctuations, the idea of *variability trend* (VT) is introduced for this purpose. From the important class of the scale-free process known as multiplicative random cascade, we show that VT exists and reveals the tree structure underlying the scale-free fluctuation. When compared to the economic and market data, similar property is found that ties the recurring trend to the scale-free property in the fluctuation.

In the next section, VT is introduced. In Sec. III, VTs from the more conventional trending features, such as polynomial and periodic trends, to that in scale-free fluctuation are shown. In Sec. IV, VTs in economic and market data are analyzed where evidence of recurring trends and the relation to the scale-free structure are presented. Concluding remarks are given in the last section.

II. VARIABILITY TREND

The main idea of our approach is to focus on the emergence of persistent trend using the increment $\Delta_d x(t)=x(t)-x(t-d)$, where $x(t)$ represents some scale-free process. Consider the mean-square increment $\Sigma\Delta_d x(t)^2/d$ in an interval of d samples. Define the difference of such increments from the past and future, respectively,

$$\Delta_d\sigma_-^2(t,T_1)=\mathcal{A}_2^-(t,d)-\mathcal{A}_1^-(t,T_1,d),$$

$$\Delta_d\sigma_+^2(t,T_2)=\mathcal{A}_2^+(t,T_2,d)-\mathcal{A}_1^+(t,d), \tag{1}$$

where $\mathcal{A}_1^-,\mathcal{A}_2^-$ denote, respectively, the mean-square increment of the past intervals $I_1^-=[t-T_1,t-T_1+d-1]$, $I_2^-=[t-d+1,t]$, and $\mathcal{A}_1^+,\mathcal{A}_2^+$ denotes, respectively, the mean-square increment of the future intervals $I_1^+=[t,t+d-1]$, $I_2^+=[t+T_2-d+1,t+T_2]$. Note that

$$A_1^-(t,T_1,d)=A_2^-(t-T_1+d-1,d),$$

$$A_1^+(t,d)=A_2^-(t+d-1,d),$$

$$A_2^+(t,T_2,d)=A_2^-(t+T_2,d). \tag{2}$$

Hence, $\Delta_d\sigma_{-,+}^2$ can be found efficiently once $A_2^-(t,d)$ is obtained.

Naturally, $\Delta_d\sigma_{-,+}^2$ involve two sets of time scales: d related to $\Delta_d x(t)$ and $T_{1,2}$ related to the fluctuation of $\Delta_d x(t)$. We call an increasing (decreasing) VT from $I_1^{-,+}$ to $I_2^{-,+}$ if $\Delta_d\sigma_{-,+}^2>0$ ($\Delta_d\sigma_{-,+}^2<0$). Define

$$U(t,T_1,T_2,d)=\Delta_d\sigma_-^2(t,T_1)\times\Delta_d\sigma_+^2(t,T_2). \tag{3}$$

Let $Y(T_1,T_2,d)=\{t,U>0\}$ record the *persistent* VT with increasing (decreasing) VT in both $I_{1,2}^-$ and $I_{1,2}^+$, and $G(T_1,T_2,d)=\{t,U<0\}$ record *alternating* VT with increasing (decreasing) VT in $I_{1,2}^-$ followed by a decreasing (increasing) VT in $I_{1,2}^+$ (Fig. 2). Finally, we estimate the relative chance of the two trends

$$\mathrm{O}(T_1,T_2,d)=(\|Y\|-\|G\|)/(\|Y\|+\|G\|), \tag{4}$$

where $\|\cdot\|$ denotes number of elements of the set.

We shall next argue in heuristic terms how a persistent trend in the fluctuation may "reveal" itself as the local maxima of O. Since I_2^-,I_1^+ are neighboring intervals, U is naturally skewed to the negative, which implies a negative O. When fluctuations in most $I_{1,2}^-$ and $I_{1,2}^+$ exhibit similar trending feature, the number of persistent VT episode increases, suggesting $\|Y\|\sim\|G\|$ and a potential local maximum $\mathrm{O}\sim 0$. When the fluctuation in most $I_{1,2}^-,I_{1,2}^+$ exhibit different trending features, the opposite $\|Y\|\ll\|G\|$ is implied, suggesting a potential local minimum of O. In much the same spirit,

 ©2009 The American Physical Society

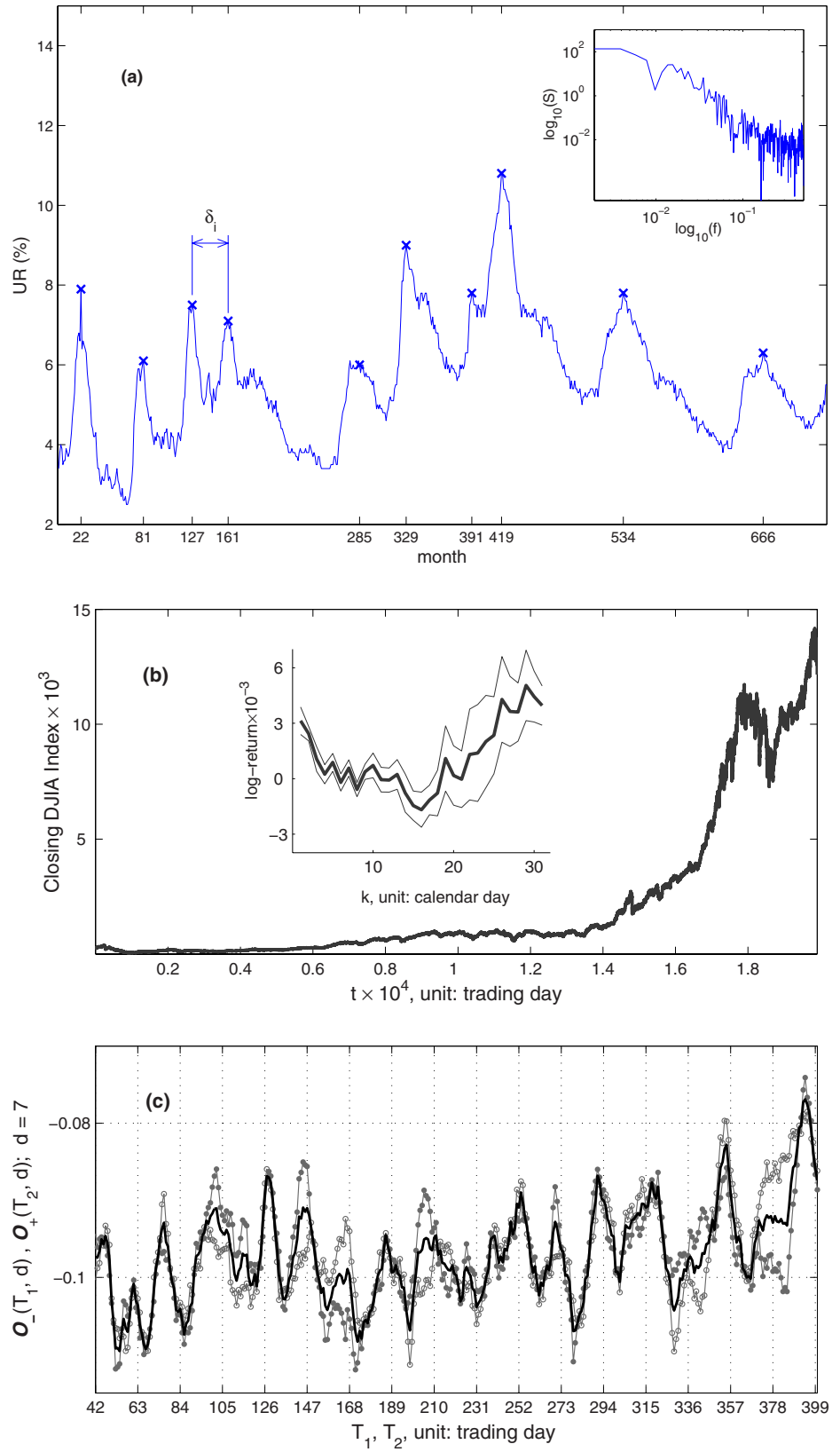

FIG. 1. (Color online) (a) Monthly UR data from 1948:01:01 to 2008:06:01 (726 months). Selected peaks are marked as × and tick marked as $\tau_1, \tau_2, \ldots$. Inset shows the $1/f$-like power spectrum. (b) Daily closing DJIA $\mathbf{D}(t)$ from 1928:10:1 to 2008:01:07 where t denotes the td. After transforming to k calendar day (c.d.), EOMR is shown in the inset based on the log-return $\mathcal{R}_d = \langle \log[\mathbf{D}(k)/\mathbf{D}(k-d)] \rangle$, $k = 1, 2, \ldots, 31$ c.d. of the month. The thin lines show ± 1 standard deviation from the scatter of $d = 1, \ldots, 10$. (c) $\mathcal{O}_-$ ("–○–"), $\mathcal{O}_+$ ("–●–"), and $\hat{\mathcal{O}}$ (thick line) at $d = 7$ td. Grid lines are drawn for every 21 td (~1 trading month).

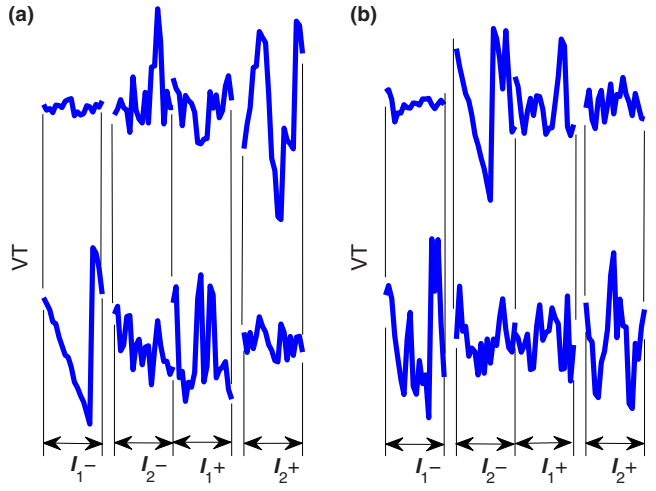

FIG. 2. (Color online) Schematics of VT: (a) two possible scenarios for persistent VT. (b) Two possible scenarios for alternating VT.

O may be thought of as a "zero-crossing" counter, except that it is aimed at capturing the persistent VT.

To capture the recurring trend, consider

$$\mathcal{O}_-(T_1,d) = \sum_{T_2} \mathrm{O}/N_2, \mathcal{O}_+(T_2,d) = \sum_{T_1} \mathrm{O}/N_1, \tag{5}$$

where $N_{1,2}$ is the number of $T_{1,2}$. From the above, the local maxima of $\mathcal{O}_-$ capture the trend in $I_{1,2}^-$ recurring in the future and the local maxima of $\mathcal{O}_+$ capture the trend in $I_{1,2}^+$ recurring in the past. As a result, recurring trends can be captured as the dominant mode of $\mathcal{O}_{-,+}$ via a spectrum calculation, $\mathcal{S}_-(f,d) = |\int \mathcal{O}_-(T_1,d)\exp(-2\pi f T_1)dT_1|^2$ and $\mathcal{S}_+(f,d) = |\int \mathcal{O}_+(T_2,d)\exp(-2\pi f T_2)dT_2|^2$.

III. VT OF ARTIFICIAL TRENDING FEATURES

In this section, we will first examine the VT of some conventional trending features to provide contrasts to the scale-free fluctuation.

A. Conventional trending features

By definition, VT is insensitive to the monotonic trending feature. For example, a polynomial trend given by $x(t) = at^n, n > 1$ implies $\Delta_d \sigma_{-,+}^2 > 0$. In this case, O=1 is simply a flat surface ($G=0$). For the linear trend in particular, U is identically zero since $\Delta_d \sigma_{-,+}^2 = 0$.

A periodic function, $x(t)=x(t+\mathrm{T})$, $\mathrm{T} \in \mathbf{R}$, represents perhaps the simplest recurring trending feature with a unique scale T. In this case, $\Delta_d \sigma_{-,+}^2$ are periodic, which implies, for $k \in \mathbf{Z}$ and any fixed T_2, $U(t,T_1+k\mathrm{T},T_2,d) = U(t,T_1,T_2,d)$ and $\mathcal{O}_-(T_1+k\mathrm{T},d) = \mathcal{O}_-(T_1,d)$. Similarly, $\mathcal{O}_+(T_2+k\mathrm{T},d) = \mathcal{O}_+(T_2,d)$. Hence, the scale of the recurring trend T is captured by the dominant mode [15] of $\mathcal{S}_{-,+}$ at $f = 1/\mathrm{T}$.

For independent and identically distributed (iid) processes, the fluctuation is trendless in that $U(t,T_1,T_2,d) = U(t,d)$ is independent of $T_{1,2}$. From the iid property, it can also be shown that U has a negative expectation. As a result, O and thus $\mathcal{O}_{-,+}$ are negative *constant* functions.

Scale-free fluctuation represents a paradigm that lies between the traditional trending features and the trendless fluctuation of the iid process. For the important class of the scale-free process known as the multiplicative random cascade (MRC), we show that recurring trending feature exists and can be effectively captured by O.

B. Variability trend in MRC

A MRC is a process defined by the product of many subprocesses varying on a range of different time scales

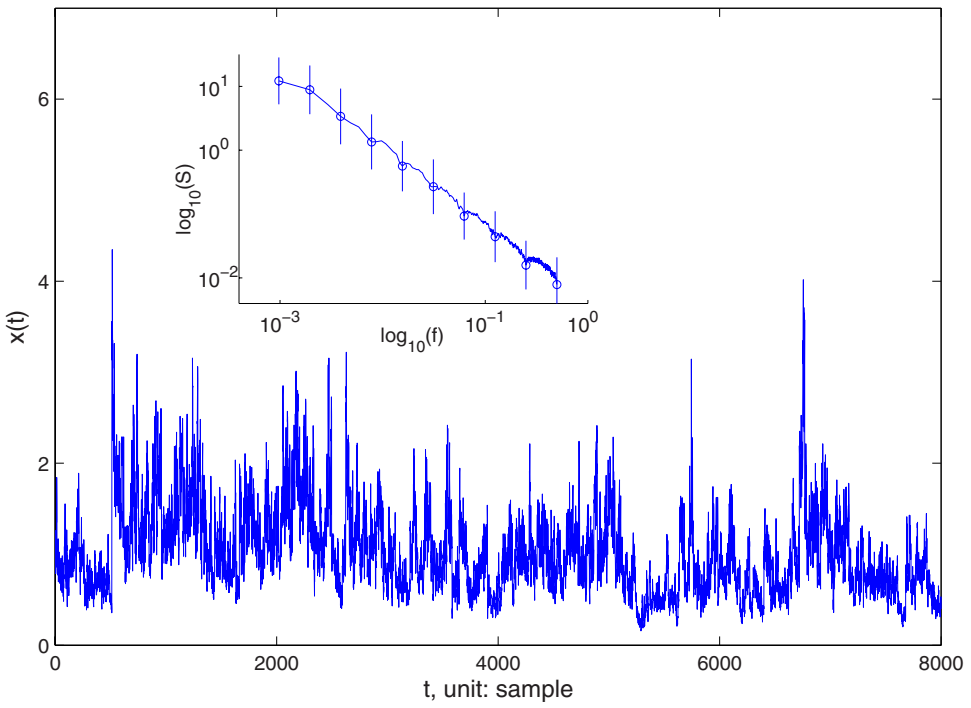

FIG. 3. (Color online) A sample of the dyadic MRC $x(t)$ and the power-law power spectrum averaged from the 100 sets of $x(t)$. Error bars of one standard deviation are shown.

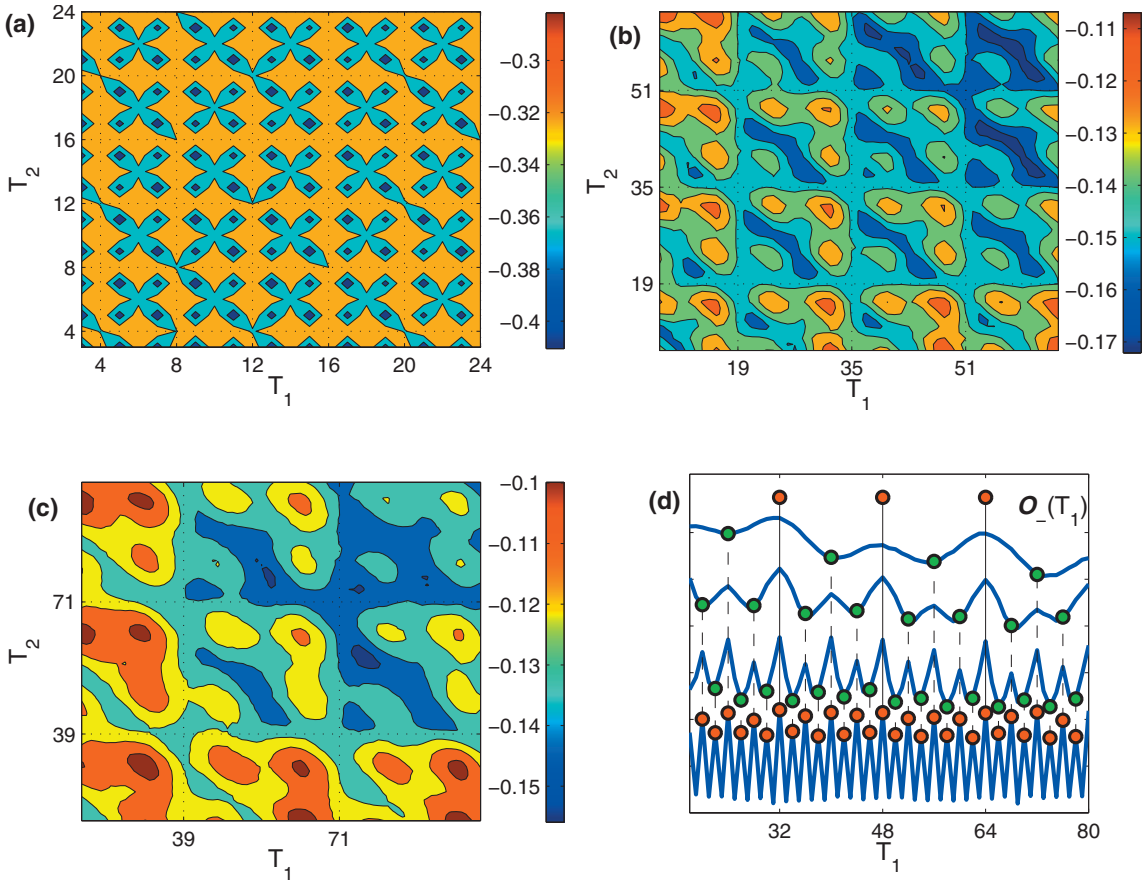

FIG. 4. (Color) Contours of O averaged over 100 sets of dyadic cascade: (a) $d=1$, (b) $d=4$, and (c) $d=8$. Six color scales from $-3\sim3$ standard deviations of the surface variation in O are used. In (d) shows $\mathcal{O}_-$ (gray) for $d=1,2,4,8$ [blue (dark grey) curves, bottom to top for clarity]. Life of local maxima from birth [red (dark grey) "○"] to death [green (light grey) "○"] are shown and guided by dashed lines. Local maxima exist beyond the analyzed d range are shown in vertical solid lines. Result from $\mathcal{O}_+$ is indistinguishable.

[16–19]. In this work, we consider $x(t)=\Pi_{j=1}^{J}\omega_j(t)$ where $\omega_j(t)>0$ is a discrete-time iid process, varying according to some law $\mathcal{L}_\omega^{(j)}$ and only at $t_k^{(j)}=kb^J/b^{j-1}$, $b\in\mathbf{Z}^+$. The set of discrete times $t^{(j)}$ forms the structure of the so-called b-adic *tree* of MRC. The tree is critical to MRC as it leads to the scale-free characteristics in the fluctuation.

To study the VT of MRC, numerical experiment is first conducted. Note, artificial $T_{1,2}$ dependence is introduced when $T_{1,2}\leq 2d-2$. Hence, only $T_{1,2}>2d-2$ should be considered. Without loss of generality, let $b=2$ (dyadic cascade). We generated 100 sets of $x(t)$ of 8192 points. Gaussian law of mean 1 and decreasing variance is used [20]: $\mathcal{L}_\omega^{(j)}=\mathbf{N}[1,2^{-2}\exp(-0.076j)]$ (Fig. 3). Figure 4 shows the ensemble average of the contour of O for $d=1,4,8$. Cell patterns are seen to emerge in intervals of $4d$ samples. They characterize the underlying tree of MRC as we now explain.

To simplify discussions, let $d=2^k$. Consider $\Delta_d\sigma_-^2$ in Eq. (1). From the dyadic tree, one can show $\mathcal{A}_2^-=\mathcal{A}_2^-[m(t,k)]$, $\mathcal{A}_1^-=\mathcal{A}_1^-[n(t,T_1,k)]$, $m,n\in[0,J-k]$, where, for $\alpha=m,n$, $\mathcal{A}_{1,2}^-(\alpha)=C_\alpha^2\Sigma_{t-d+1}^{t}(\Pi_{\alpha+1}^{J}\omega_j)^2$, $C_\alpha(t)=\Pi_1^\alpha\omega_j(t)$ (the dependent variable "t" will be suppressed). For $k\ll J$, C_α^2 is the dominant factor of $\mathcal{A}_{1,2}^-(\alpha)$. The cell pattern can thus be analyzed by m,n as functions of t,T_1. Consider first $m(t,k)$ in $\mathcal{A}_2^-$. Denote $A,B,C,D,\ldots$ as $J-(k+1)$, $J-(k+2)$, $J-(k+3)$, $J-(k+4)$,…, respectively. Due to the dyadic tree, there is a one-to-one correspondence between the set $\{m(t,k),t=1,2,\ldots\}$ and the symbolic sequence made up of sub-blocks of $2d$ samples and of the form $A\gamma\cdots\gamma$, $\gamma=B,C,D,\ldots$,

$$\{\cdots AB\cdots BAC\cdots CAB\cdots BAD\cdots DAB\cdots BAC\cdots C\cdots\}. \tag{6}$$

More, $\Theta=AB\cdots B$ in Eq. (6) is a periodic block of period $4d$ and, for $m\in\Theta$,

$$\mathcal{A}_2^-(m)=C_{J-(k+2)}^2\sum_{t'=t-d+1}^{t}\left[\prod_{J-(k+1)}^{J}\omega_j(t')^2\right].$$

Similarly for $\mathcal{A}_1^-$, $\{n(t,T_1,k),t=1,2,\ldots\}$ is given by Eq. (6) shifted T_1-d+1 samples to the right. When the shift equals $l4d,l\in\mathbf{Z}$, the segments corresponding to Θ in $\mathcal{A}_{1,2}^-$ line up perfectly. Their difference creates in $\Delta_d\sigma_-^2(t,T_1)$ segments of statistically identical property, repeating for every $4d$ samples. In what follows, these segments are referred to as the $\delta\Theta$ segments.

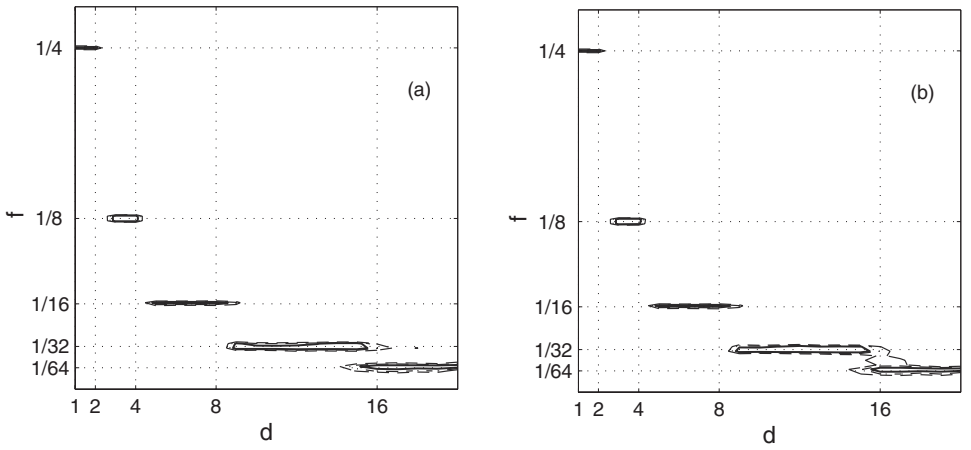

FIG. 5. Contour configuration $\{(d,f),\hat{S}(f,d)=C_0\}$ averaged over (a) 50 and (b) 100 sets of dyadic cascade: $C_0=0.7$ ("- -"), $C_0=0.8$ ("– -"), and $C_0=0.95$ ("–"). Note the contour lines of $C=0.7,0.8$ almost overlap.

The $\Delta_d\sigma_+^2$ is analyzed the same with the same $\delta\Theta$ segments emerging at $T_2=l'4d+(d-1)$, $l'\in\mathbf{Z}$. By Eq. (3), $U=\Delta_d\sigma_-^2\Delta_d\sigma_+^2$, the product of the $\delta\Theta$ segments thus implies persistent VT. Its period of $4d$ implies the cell pattern seen in Fig. 4. Note that longer periodic blocks other than Θ exist. These additional "modes" contribute to the changing pattern in the cells.

Given $T_{1,2}$, the local maxima of $\mathcal{O}_{-,+}$ can be estimated based on the number of persistent VT in U. For example, by Eqs. (3) and (6), a straightforward counting shows $\sim N/8$ persistent VTs for $T_1=2d$, $T_2=8d$ or $\sim N/2$ persistent VTs for $T_{1,2}=8d,8d$, where N is the number of data points. For MRC, one can show the local maxima of $\mathcal{O}_{-,+}$ at $T_{1,2}^*=l2^{k+1}$, $l'2^{k+1}$ for $d\in(2^{k-1},2^k]$ and integers $l,l',k>1$. Results for $d=1,2,4,8$ are shown in Fig. 4(d).

Two observations can be made that show the distinct VT characteristics of MRC: (a) the local maxima are perfectly aligned and only exists for a *finite* d range and (b) by arranging $\mathcal{O}_{-,+}$ vertically from small to large d, the tree of MRC can be traced out by connecting the local maxima from "birth" to "death" [Fig. 4(d)]. The emergence of the tree structure in Fig. 4(d) makes sense in that the averaging in obtaining the mean-square increment "washes out" the variability of scales $<d$ so U only fluctuates according to the "next in scale" of the tree built recursively in the cascade.

The ability to track the tree provides the opportunity to systematically examine similar structures in the empirical data. This may be achieved by tracking the dominant modes of $\mathcal{S}_{-,+}$. Since the variability of scale $<d$ is averaged in the mean-square process (1), medium to high-frequency modes are suppressed in $\mathcal{O}_{-,+}$ as d increases. As a result, the modes of $\mathcal{S}_{-,+}$ can be buried in the broad band fluctuation of $\mathcal{O}_{-,+}$ as d increases. To extract the dominant modes in practice, we first delete a polynomial trend in $\mathcal{S}_{-,+}$. In addition, to properly reveal and compare the dominant modes for a range of d, $\mathcal{S}_{-,+}$ is further normalized according to $\max(\mathcal{S}_{-,+})=1$.

Take the MRC as an example. The dominant modes of $\mathcal{S}_{-,+}$ are located at $f=1/2^{k+1}$ for $d\in(2^{k-1},2^k]$. Hence, the persistent VT is translated into persistent modes of $\mathcal{S}_{-,+}$ as a function of d. On the $d\times f$ plane, the level set $\{(d,f),\mathcal{S}_{-,+}$

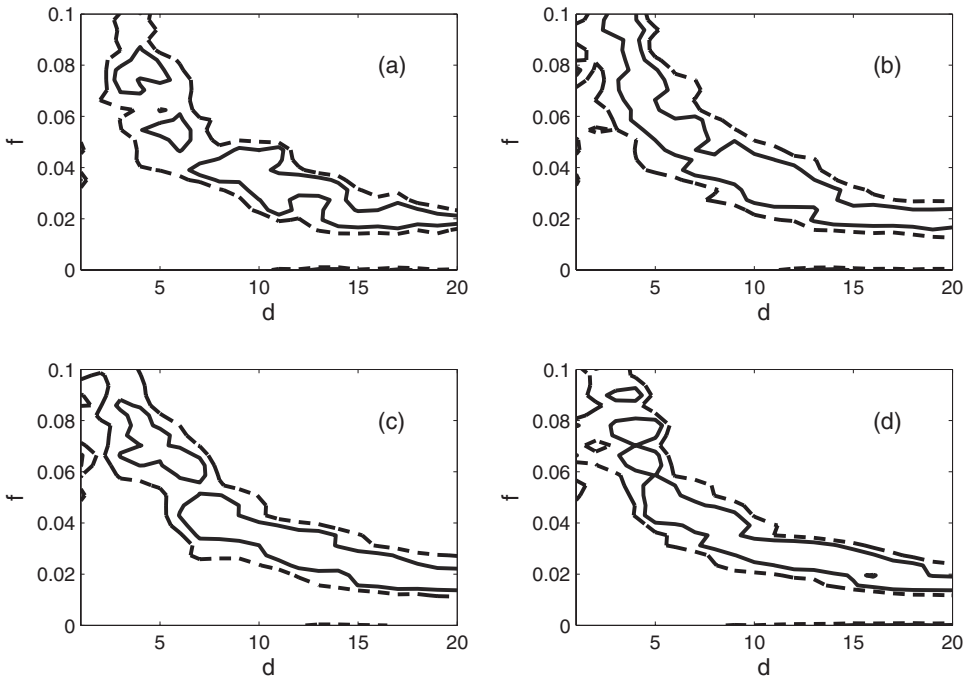

FIG. 6. Contour configuration $\{(d,f),\mathcal{S}_{(f,d)}=C_0\}$ of fBm for $C_0=0.7$ (long-dashed line) and $C_0=0.9$ (dark line): (a) $H=0.2$ averaged over 50 sets, (b) $H=0.2$ averaged over 100 sets, (c) $H=0.5$ averaged over 100 sets, and (d) $H=0.8$ averaged over 100 sets.

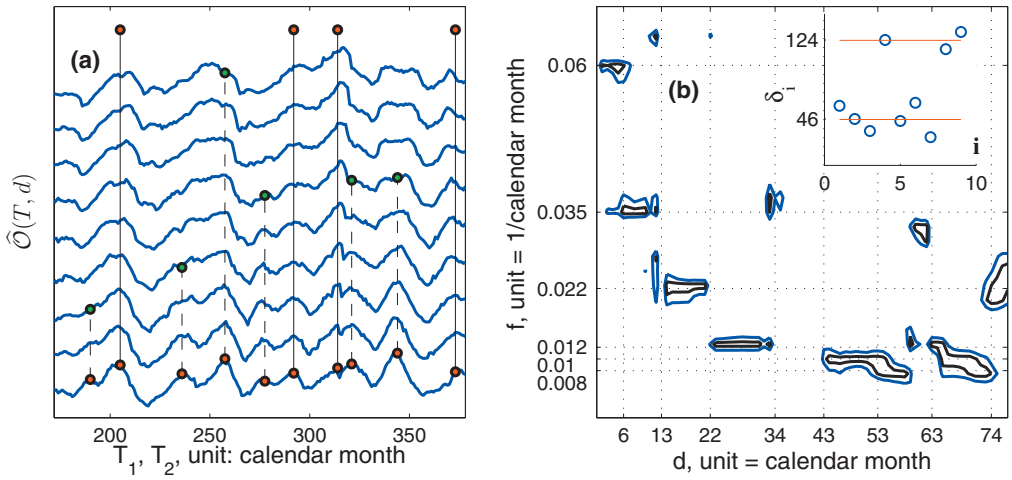

FIG. 7. (Color) (a) $\hat{\mathcal{O}}(T,d)$ of UR data, $d=8,\ldots,16$ (arranged bottom to top). For illustration, (small) linear trend was deleted. Guided solid and dashed lines are added in the neighborhood of local maxima of $\hat{\mathcal{O}}$. The birth and death locations of the local maxima are shown in solid circles. (b) Contour configuration $\{(d,f),\hat{\mathcal{S}}(f,d)=C_0\}$ calculated for each d shown in (a) $C_0=0.7$ (blue line) and 0.9 (dark line). Specific scales mentioned in the text are tick marked. Inset shows the δ_i, the duration between selected UR peaks ($\times$) in Fig. 1(a). The averaged δ_i over the two bands are drawn in lines (see text).

$=C_0\}$ reveals a step-wise descending contour configuration of the dominant modes that is particular to the underlying tree (Fig. 5). Such a pattern quickly stablizes as ensemble size increases the averaging process. This provides a clear contrast to the other scale-free fluctuation we discuss next.

C. Other scale-free fluctuation

In general, there are also scale-free processes that do not prescribe to a tree structure. In this section, we shall examine the example of fractional Brownian motion (fBm) which has a continuous scale-free property. In this case, we will show that the distribution of dominant modes in $\mathcal{S}_{-,+}$ is qualitatively different.

By definition [21], a fBm $x(t)$ is a stochastic process that is continuous with probability 1 and has a stationary Gaussian increment,

$$\text{Prob}[x(t)-x(t-d)\le z]=(2\pi d^{2H})^{-1/2}\int_{-\infty}^{z}\exp(-u^2/2d^{2H})du, \tag{7}$$

where H is known as the Hurst exponent. Without loss of generality, let $x(0)=0$, and Eq. (7) implies, for *any* $d\in\mathbf{R}$, that

$$x(dt)=^{\text{law}}d^{-H}x(t), \tag{8}$$

where $=^{\text{law}}$ means identical in law. Hence, $x(t)$ is self-similar and lacks an absolute scale for its characterization. One may synthesize fBm by randomizing the Weierstrass function or by using the wavelet transform [21]. Unlike MRC, the synthesis of fBm does not involve a tree construct. As a result, the persistent VT in fBm scatters does not exhibit any recurring trend.

To show this numerically, we simulate 100 sets of $x(t)$ of 2000 points for $H=0.2,0.5,0.8$. For each $x(t)$ in the ensemble, the VT is analyzed for $T_{1,2}\in[2d,256]$ and the results ensemble averaged to obtain the $\mathcal{O}_{-,+}$. The contour configuration of the dominant modes of $\mathcal{S}_-$ for $d\in[1,20]$ are shown in Fig. 6 ($\mathcal{S}_+$ is similar and not shown). The dominant modes for fBm are seen to reside over a continuous band on the $d\times f$ plane. We also found that the larger the ensemble size is, the clearer this pattern develops [Figs. 6(a) and 6(b)]. In contrast, the contour configuration of MRC shows little

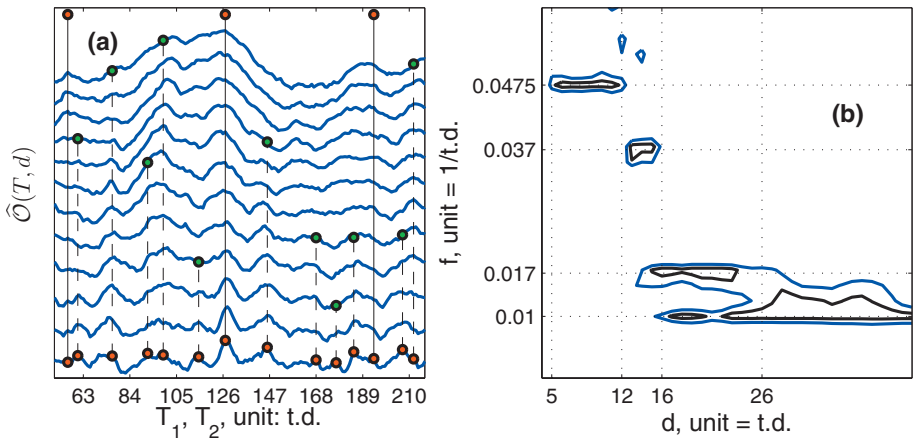

FIG. 8. (Color) (a) $\hat{\mathcal{O}}(T,d)$ from daily DJIA, $d=5,\ldots,16$ (arranged bottom to top). Guided solid and dashed lines are shown in the neighborhood of local maxima of $\hat{\mathcal{O}}$ with the same labeling as Fig. 7(a). Note that $d=7$ (third curve from the bottom) is the same as Fig. 1(c). (b) Contour configuration $\{(d,f),\hat{\mathcal{S}}(f,d)=C_0\}$ calculated for each d shown in (a) $C_0=0.7$ (blue line) and 0.9 (dark line). Specific scales mentioned in the text are tick marked.

variation with the ensemble size [Figs. 5(a) and 5(b)]. This comparison demonstrates the unique property in the scale-free fluctuation derived from a treelike structure.

IV. VARIABILITY TREND OF ECONOMIC AND MARKET DATA

For the empirical data, the average $\hat{\mathcal{O}}=(\mathcal{O}_-+\mathcal{O}_+)/2$ is used since $\mathcal{O}_{-,+}$ are not significantly different. Figure 7(a) shows the $\hat{\mathcal{O}}$ from UR data [Fig. 1(a)]. The local maxima show a "fractured" but similar configuration as the cascade's. The spectral density of $\hat{\mathcal{O}}$ is calculated as a function of frequency and d, $\hat{\mathcal{S}}(f,d)=|\int\hat{\mathcal{O}}(T,d)\exp(-2\pi fT)dT|^2$. The step-wise descending contour configuration found in MRC (Fig. 5) is clearly present in the UR data [Fig. 7(b)]. The dominant modes are estimated at $f=0.008,0.01,0.012,0.022,0.035,0.06$ (1/month). These numeric values suggest severe economic downturns recurred at the time scales ~17, 29, 45, 83, 100, and 125 (month) or ~1.4, 2.4, 3.8, 6.9, 8.3, and 10.4 years.

To match the evidence in the data, let $\tau_1,\tau_2,\ldots$ be selected at easily recognized peak locations of the UR data ["×" in Fig. 1(a)]. The intervals $\delta_i=\tau_{i+1}-\tau_i$ are found to lie in two bands (28, 60) and (115, 140). The δ_i in the two bands are averaged to ~46 124 (month) consistent with the estimates from $\hat{\mathcal{S}}$. Since these peaks reveal the recurring trend of UR, the structure implied from $\hat{\mathcal{S}}$ suggests that some treelike structure likely underlies the recursive nature of economic downturns.

As a second application, we turn to the EOMR trend in the daily closing index of Dow Jones Industrial Average (DJIA) [Fig. 1(b)]. The fluctuation in DJIA has been reported in many studies [6–8]. Again, the local maxima of $\hat{\mathcal{O}}$ show fractured but similar characteristics as the cascade [Fig. 8(a)]. In this case, the connection to the trending feature of EOMR is immediate. For example, for $d=7$ trading days (td), local maxima are mostly separated in intervals of ~21 td (~1 trading month), matching the characteristic of EOMR [see Fig. 1(b)]. The dominant modes estimated from $\hat{\mathcal{S}}$ also show the similar step-wise descending pattern as d increases [Fig. 8(b)]. These modes are located at $f\sim0.01,0.017,0.037,0.048$ (1/month) or ~100,59,27,21 td. Similar to the UR interpretation, these dominant modes of $\hat{\mathcal{S}}$ suggest that the EOMR phenomenon is likely a manifestation of certain multiple scaling structure rather than the presence of Fourier mode(s).

To tentatively compare to the dominant modes of MRC, gaps are observed in the treelike object of UR data. They are found in the intervals $d\in(34,43)$ and (59,63), which averaged to ~3.2 and ~5.1 years, respectively. In the gap regions, a different set of dominant modes is seen to emerge outside the contour configuration. For DJIA, the treelike object seems more "intact" and the transition between the dominant modes can be estimated at $d\sim5$, 12, 16, and 26 td.

V. CONCLUDING REMARKS

The notion of trend in the scale-free fluctuation is defined and systematically examined based on the idea of VT and the relative increase in persistent VT episode. From MRC and empirical data, a plausible scenario emerges, which relates the recurring trend to the scale-free structure of the fluctuation. In particular, we suggest that the localized treelike structure underlies the trending feature in the scale-free fluctuation; i.e., rather than an aberration, the recurring trend is a manifestation and an integral part of the scale-free fluctuation.

While the analyzed data share the similar VT structure as MRC, their details appear to be more complex. It is plausible that multiple treelike structures are present. For example, Fig. 7(a) shows the "splitting" of a local maxima at $T\sim340$ and $d\sim12$ (sixth curve from the bottom), suggesting the possible birth of a new cascade. Note that this also coincides with the additional mode identified in the gap region mentioned above. Finally, the more "recognizable" trending feature in UR could suggest similar cascade subprocesses underlying the treelike object in severe economic downturns. In contrast, the recurring VT of MRC, while shown to exist, is not discernible from the raw data.

It is of interest to compare to other frequency domain approach. As discussed in the introduction, the Fourier transform of the raw data reveals only the $1/f$-like power-law spectrum. As shown in this study, the fluctuation of MRC does contain certain "phase" information that is closely related to the underlying tree, i.e., the cell pattern in Fig. 4. The result of Fourier or similar integral transform is largely based on the random amplitude of the fluctuation data. The alternative to using VT provides the chance to extract this phase information. This comment also applies to the wavelet approach which is an integral transform that relies on the fit of the mother wavelet to the data. But we should mention the similar effect that the so-called wavelet transform modulus maxima method is able to achieve when applied to a deterministic cascade (Cantor set) [see, for example, Fig. 1d in Ref. [22]]. However, it becomes quickly ineffective to extract the tree structure when applied to MRC.

For a more detailed understanding of the scale-free fluctuation and the recurring trend, modeling in reference to the specific market variables is necessary. The main implication of the current study is that these two characteristics may have to be modeled as a whole rather than separate elements of the dynamics. More general questions such as the initiation and organization, if any, of multiple treelike structures in scale-free fluctuation are the challenges in the future work.

ACKNOWLEDGMENT

This research is supported by the Natural Science and Engineering Research Council of Canada.

[1] T. Gisiger, Biol. Rev. Cambridge Philos. Soc. **76**, 161 (2001), and references therein.
[2] M. M. Dacorogna, U. A. Muller, R. B. Olsen, and O. V. Pictet, Quant. Finance **1**, 198 (2001).
[3] T. Di Matteo, Quant. Finance **7**, 21 (2007).
[4] B. Mandelbrot, J. Business **40**, 393 (1967).
[5] B. B. Mandelbrot, *Fractals and Scaling in Finance* (Springer, New York, 1997).
[6] R. N. Mantegna and H. E. Stanley, Nature (London) **376**, 46 (1995).
[7] K. Ivanova and M. Ausloos, Eur. Phys. J. B **8**, 665 (1999).
[8] C. Ellis and C. Hudson, Physica A **378**, 374 (2007).
[9] T. Lux and M. Marchesi, Nature (London) **397**, 498 (1999).
[10] T. Lux, Physica A **15**, 481 (2004).
[11] A. A. Christie, J. Financ. Econ. **10**, 407 (1982).
[12] J. Yu, J. Econometr. **127**, 165 (2005).
[13] J. Lakonishok and S. Smidt, Rev. Financ. Stud. **1**, 403 (1988).
[14] W. Xu and J. J. McConnell, Financ. Anal. J. **64**, 49 (2008).
[15] Since the increment is squared, the dominant mode of $\mathcal{O}_{-,+}$ can emerge at a scale smaller than T. Take $x(t)=\sin(t/\mathrm{T})$. Its dominant mode is identified at the scale T/2 due to the exact mirror symmetry of the harmonic function about its half period point.
[16] B. B. Mandelbrot, J. Fluid Mech. **62**, 331 (1974).
[17] P. Collet and F. Koukiou, Commun. Math. Phys. **147**, 329 (1992).
[18] G. M. Molchan, Commun. Math. Phys. **179**, 681 (1996).
[19] M. Ossiander and E. C. Waymire, Ann. Stat. **28**, 1533 (2000).
[20] The same result is obtained for using Gaussian laws of identical variance.
[21] K. Falconer, *Fractal Geometry* (John Wiley & Sons, New York, 1990).
[22] A. Arneodo, E. Bacry, and J. F. Muzy, Physica A **213**, 232 (1995).